Scaling relationships for strip fibre reinforced aggregates

Olufemi Ajayi

Louis Le Pen

Antonis Zervos

William Powrie

Faculty of Engineering and the Environment, University of Southampton, Southampton SO17 1BJ, United Kingdom

23 November 2016

Abstract

Previous research on random fibre reinforced granular materials has shown that the relative dimensions of the grains and fibres significantly affect the macro-mechanical behaviour of the mixture. However, quantitative data are scarce and most previous work has focused on fine to medium sands, leaving uncertainties regarding the applicability of current knowledge to larger size aggregates such as railway ballast. In this paper, triaxial test data on $^1/_3$ and $^1/_5$ scale railway ballast are used to develop scaling relationships for the size and quantity of fibres needed to achieve the same reinforcing effect in granular materials of differing grain size. It is shown that, to maintain consistency across scales, fibre content should be quantified as a numerical (i.e. number of fibres per grain) rather than a volumetric ratio. It is further shown that increasing the fibre length increases the resistance of the mixture to deviator stress if the fibres are wide enough; and that provided an allowance is made for the effect of fibre tension, the changes in the stress-strain-strength behaviour of the granular matrix resulting from the changes in void ratio associated with the addition of the fibres are consistent with conventional soil mechanics theory across scales.

Keywords: Fibre reinforcements, Granular materials, Railway ballast, Scaling relationships

List of symbols

D_{50} - mean grain size

e - void ratio

E_f - fibre Young's modulus

I_D - density index

L_f - fibre length

L_N - normalized length

N_f - number of individual fibres

N_{fg} - fibre:grain ratio

N_g - average number of grains

p - mean effective stress

p'' - corrected mean effective stress

q - deviator stress

q'' - corrected deviator stress

t_f - fibre thickness

V_f - volume of fibres

V_{fr} - volumetric fibre ratio

V_s - volume of the grains (or "solids")

V_v - volume of voids

W_f - fibre width

W_N - normalized width

α - fibre/grain interaction factor

ε_a - axial strain

ε_r - radial strain

ε_{vol} - volumetric strain

η - stress ratio

σ'_3 - radial stress

σ''_3 - corrected lateral stress

σ'_f - additional lateral stress

Introduction and background

It is well-known that the strength and ductility of a sand can be improved by the addition of randomly-distributed fabric, polymer or metal fibres (e.g. Michalowski and Cermak, 2002; Lirer et al., 2011; Diambra et al., 2013). Initial tests on much larger-grained, scaled and full-sized railway ballast show similar promise (Abadi, 2015). The mechanical behaviour of the reinforced material depends on the properties of both the fibres and the grains, as well as their relative sizes and proportions (e.g. Michalowski and Cermak, 2003; Sadek et al., 2010).

Michalowski (1997) identified two alternative sand-fibre interaction mechanisms, related to the relative effective diameters of the grains and the fibres:

1. Where the representative diameter of the soil grains D_{50} (the median grain size of soil by weight) is small in comparison with the effective fibre diameter D_f, the number of grain contacts area for an individual fibre is relatively large and the frictional fibre-grain matrix interface may be considered continuous. This is the approach used with soil nails, which may be viewed as a particular case of soil reinforcement. It is termed *short fibre reinforcement* by Michalowski (1997), although the real point is that the fibre diameter is larger than the typical grain size, i.e. $D_N = D_f/D_{50} > 1$, where D_N is the normalised fibre diameter:

2. Where the diameter of the fibre is at least an order of magnitude smaller than the median grain size, i.e. $D_N < 0.1$, individual contacts and the way in which the fibres fit into the pore space may need to be considered at the grain scale. This is termed *continuous thin filament fibre reinforcement* by Michalowski (1997). Michalowski (1997) also states that this mechanism of reinforcement relies on the development of a force in each fibre as a result of a "belt-friction effect", as the fibre wraps around the grains. The fibre must therefore be rather longer than the typical grain size, i.e. $L_f >> D_{50}$, where L_f is the fibre length. Allowing for a fibre to wrap fully round two adjacent grains requires $L_f > (2\pi + 1) \times D_{50}$. This is approximately one order of magnitude, implying $L_N = L_f/D_{50} \geq 10$, where L_N is the normalised fibre length.

It is clear from the foregoing that, notwithstanding the nomenclature adopted by Michalowski (1997), the mechanism of fibre reinforcement depends on the length and thickness of the fibres relative to the grains, as well as on the amount of fibres present and their bending stiffness. The aim of this paper is to develop the understanding of the impacts of the relative fibre:grain dimensions and the proportion of fibres present on the mechanical behaviour of a coarse granular material, in the context of using fibre reinforcement to improve the performance of a scaled railway ballast.

Ballast is a main component of a traditional railway track system. It resists and distributes the vertical, lateral and longitudinal forces applied to the track by trains as they pass, curve, brake and accelerate. In response to the many millions of loading cycles it experiences, ballast generally undergoes gradual plastic settlement. Such settlement, especially if it is differential, causes a loss of track geometry (level and line) and can result in the imposition of speed restrictions and/or a requirement for emergency remediation. The benefits of using geogrids to reinforce railway ballast, in reducing both lateral spread and vertical settlement, are reasonably well established (e.g. Bathurst and Raymond, 1987; McDowell et al., 2006; Indraratna et al., 2010; Indraratna et al., 2011). However, a drawback of that approach is the restriction it imposes on future maintenance activities - particularly tamping, which would disrupt or destroy the geogrids if they were placed in the tamped zone. The addition of randomly distributed synthetic fibres could provide an alternative way of reinforcing ballast that is able to withstand typical tamping operations, permitting reinforcement through the full depth.

Although some results from a well-graded gravel with grain sizes in the range 0.2 – 10 mm were reported by Lirer et al. (2011), research on fibre reinforced granular materials has to date focused mainly on fine to medium sands. Thus neither the effect of fibre reinforcement on larger grained aggregates, nor the relevant underlying mechanisms of grain-fibre interaction have been fully investigated. It is reasonable to expect that both the effects and the micromechanics will be similar, provided that the fibre dimensions are appropriately scaled to account for the larger grain size. However, the ways in which the fibre-grain interactions influence the improvement in sand behaviour scale with grain size are uncertain.

This paper reports the results of an investigation into the mechanical properties of fibre reinforced granular materials representing ⅓ and ⅕ scale railway ballast. Particular emphasis is placed on the effects of fibre content, as well as the relative dimensions of the fibres and grains, for the different grain size ranges. Relationships are developed for the size and quantity of fibres required to achieve the same reinforcing effect in granular materials of different grain sizes.

Experimental work

Materials

Testing of scaled ballast (SB) offers an attractive way of developing an understanding of the mechanics of the full size material. Direct testing of the latter is difficult and can be unreliable, owing to the challenges that the large grain size creates for laboratory element tests. For a given aggregate, measurable variations in grain shape occur

with grain size over a range of sieve intervals. However, these variations are relatively slight (Sevi, 2008; Le Pen et al., 2013). Thus tests on scaled ballast have been used to investigate the development of plastic deformation under cyclic loading (Sevi et al., 2009), deformation under a moving wheel load (Ishikawa et al., 2011), and the contribution of the ballast shoulder to the resistance of a railway sleeper to lateral movement (Koike et al., 2014; Le Pen et al., 2014). Triaxial tests on the scaled ballast and on full size ballast in a testing apparatus representing an element of track have shown that the particular granite ballast used was not susceptible to breakage for cyclic stress paths representative of train loading (Aingaran, 2014; Abadi et al., 2016).

Two granular materials (scaled ballasts) of different grain sizes were used in this work. Both were crushed granite from the same quarry, with gradations parallel to that of a typical railway ballast at $^1/_5$ and $^1/_3$ of the full size (Figure 1). The reinforcement comprised tape-like polyethylene fibres or strips (Figure 2), cut to size from damp proof course (DPC) material with a light texture embossed on its surface. The textured surface of the fibres was relatively smooth, hence was not considered explicitly in the interpretation of the laboratory test results. The mechanical properties of the fibres are summarised in Table 1.

Phase relations and initial specimen density

Relationships between the phases (voids, fibres and grains) are defined using the following parameters,

Void ratio (e): the ratio of the volume of voids (V_v) to the volume of the grains (or "solids"), (V_s)

$$e = \frac{V_v}{V_s} \tag{1}$$

Volumetric fibre ratio (V_{fr}): the ratio of the volume of fibres (V_f) to the volume of solids, V_s

$$V_{fr} = \frac{V_f}{V_s} \tag{2}$$

These consider the fibres independently of both the solids and the voids, with V_s as the common denominator. However, they do not differentiate between voids associated with the grains and voids associated with fibres. The relative density index I_D is defined in the conventional way, on the basis of the maximum and minimum void ratios e_{max} and e_{min} attainable with the unreinforced granular material.

$$I_D = \frac{e_{\max} - e}{e_{\max} - e_{\min}} \tag{3}$$

where e_{max} and e_{min} are the maximum and minimum void ratios for the unreinforced scaled ballast. As noted by Ajayi et al. (2016), this means that values of I_D for the reinforced materials may be negative because of the disruptive effect of the fibres on grain packing.

Fibre reinforced scaled ballast was prepared by hand-mixing known masses of fibres and scaled ballast grains in a plastic container. The resulting distribution of fibres was reasonably uniform. Fibre orientation was mostly sub-horizontal, generally within the range of ±30° to the horizontal plane reported by Diambra et al. (2008). The maximum and minimum void ratios (e_{max} and e_{min}) achievable using the methods of compaction and placement described by Ajayi et al. (2016) increased with increasing V_{fr}, indicating that the addition of fibres interferes with the packing of the grains. This corroborates the findings of others including Michalowski and Zhao (1996), Ibraim and Fourmont (2007) and Dos Santos et al. (2010).

Fibre dimensions and fibre content

To compare the effects of fibre reinforcement across two scales of ballast ($^1/_5$ and $^1/_3$), the triaxial test results are reported in terms of relative fibre/grain dimensions. The relative fibre to grain dimensions are referred to as the normalized length and width (L_N and W_N), given by

$$L_N = \frac{L_f}{D_{50}} \tag{4}$$

$$W_N = \frac{W_f}{D_{50}} \tag{5}$$

where L_f is the fibre length, W_f is the fibre width and D_{50} is the mean grain size of the granular medium. The normalized dimensions of the materials used in the triaxial tests are summarised in Table 2.

Assuming that all grains are approximately spherical with a diameter equal to the median grain size D_{50}, the number of grains (N_g) in a fibre reinforced specimen may be estimated. The number of individual fibres (N_f) in a specimen is relatively small and can be counted visually. The ratio of the number of fibres to the number of grains is then referred to as the fibre:grain ratio N_{fg}.

$$N_{fg} = \frac{N_f}{N_g} \tag{6}$$

The values of N_{fg} for each of the materials tested are shown in Table 2. The fibre thickness was not changed, and it is assumed that the individual fibres remained flexible, (i.e. that their bending stiffness, which will increase with fibre thickness, was not significant).

Test apparatus and procedure

Triaxial tests were carried out on 150 mm diameter × 300 mm high specimens in a strain-controlled triaxial apparatus. Global axial displacement was measured using a displacement transducer (LVDT) located on top of the triaxial cell, and the axial force using an internal load cell. Local instrumentation was not attached to the specimens owing to the erratic nature of measurements resulting from random movements of the relatively large grains and because the strains for typical railway ballast tested to failure are large enough for the global axial displacement transducer to measure reliably (Atkinson, 2000).

A transducer attached to the cell pressure inlet measured the cell pressure being applied to the specimen. The triaxial tests were carried out on dry specimens internally open to the atmosphere, i.e. without the application of a back pressure. Volume change was measured by the cell pressure controller. This is shown by Ajayi et al. (2016) to give results within ±1 % of those using the pore pressure controller in a drained test on a saturated specimen. Pressure and volume were measured to a resolution of 0.1 kPa and 1 mm^3 respectively.

Reinforced and dense unreinforced scaled ballast triaxial test specimens were prepared by placing known quantities of previously hand-mixed fibres and grains within a split cell mould lined with a rubber membrane, followed by vibratory compaction under a 5 kg surcharge. The unreinforced loose specimen was prepared by placing a long, 100 mm diameter tube, open at both ends, upright in a split mould on the triaxial pedestal. Sufficient scaled ballast to fill the mould was then placed into the tube and the tube was slowly lifted, so that the scaled ballast grains descended gently into the mould. The triaxial tests were carried out at a cell pressure of 30 kPa, which is at the likely upper end of the range of lateral stresses within railway ballast (e.g. Indraratna et al., 2010; Sevi and Ge, 2012). The cell pressure was kept constant during shear and the influence of varying the cell pressure was not studied in these tests. The triaxial tests reported and the initial conditions for each specimen are summarised in Table 2.

Test results and analysis

Interpretative framework

It is generally accepted that the improved mechanical behaviour of long-fibre reinforced granular materials arises from the development of tension in the fibres. Following Jewell and Wroth (1987), Ajayi et al. (2016) show that, if this fibre tension is accounted for by means of an additional effective stress acting on the soil grains, the stress-strain-strength behaviour of the granular matrix conforms to the established principles of soil mechanics. That is, the limiting corrected effective stress ratio is not altered by the addition of fibres, and the volume-related behaviour (particularly the increased ductility, reduced tendency to dilate, and the achievement of a peak stress ratio) is consistent with the increase in the void ratio caused or enabled by the fibres.

The enhancement to the effective radial stress experienced by the granular skeleton at a radial strain ε_r as derived in Ajayi et al. (2016) is

$$\frac{F}{A} = \sigma'_f = \frac{\alpha \cdot \varepsilon_r \cdot E_f \cdot V_{fr}}{\left(1 + e + V_{fr}\right)} \tag{7}$$

where α is a fibre/grain interaction factor which accounts for the fibre orientation, fibre slippage and fibre end effects, and E_f is the fibre Young's modulus.

The fibre/grain interaction factor α may vary with strain and is assumed to take the form,

$$\alpha = A_\alpha \left|\varepsilon_r\right|^{-B_\alpha} \tag{8}$$

where A_α and B_α are constants for a given combination of granular material, fibre type, fibre geometry and fibre content (Ajayi et al., 2016). The fibre/grain interaction factor α must be in the range $0 \leq \alpha \leq 1$. The values of A_α and B_α are determined by curve fitting so that the stress-dilatancy behaviours of the granular matrix in true effective stress terms were the same for each material type. The evolution of σ'_f with axial strain for $^1/_3$ and $^1/_5$ scale ballast specimens with different V_{fr} is shown in Figure 3.

The corrected radial (lateral) stress on the granular skeleton, denoted σ''_3, is then (Ajayi et al., 2016)

$$\sigma''_3 = \sigma'_3 + \sigma'_f \tag{9}$$

This additional effective stress acts only in the radial direction, partly because the axial stress is compressive and it is assumed that the fibres have no stiffness in compression, and partly because the orientation of the fibres is substantially horizontal.

The corrected deviator stress, q'', and the corrected mean effective stress, p'', then become (Ajayi et al., 2016)

$$q'' = q - \sigma'_f \tag{10}$$

$$p'' = \frac{1}{3}\left(\sigma_1'' + 2\sigma_3''\right) = p' + \frac{2}{3}\sigma'_f \tag{11}$$

However, presenting the results in this way masks the benefit of fibre reinforcement in terms of the increase in the peak deviator stress achieved. Hence the results will be presented and discussed initially in terms of total deviator stress, axial and volumetric strain. It must be emphasised that the total deviator stress and the cell pressure do not reflect the true effective stresses experienced by the granular skeleton. Where appropriate, data are also presented and discussed in terms of the true effective stresses given by Eqs (10) and (11).

Effects of L_N and W_N

Figure 4 shows graphs of deviator stress q and volumetric strain ε_{vol} against axial strain ε_a for triaxial tests on unreinforced $^1/_5$ and $^1/_3$ scale ballast, demonstrating the similiarity in their mechanical behaviour.

Owing to the larger particle sizes being considered in this work, it is reasonable to expect that the influence of the relative fibre dimensions on the macro-mechanical behaviour will be more pronounced than with a sand. The effects of changing L_N and W_N will now be considered.

Figure 5 shows the evolution of the additional effective lateral stress σ'_f with axial strain for specimens having different L_N and W_N and the same fibre content (V_{fr} = 1.6%). Figure 5 suggests that increasing W_N provided L_N is long enough, or increasing L_N provided that W_N is wide enough for significant fibre-grain interaction to take place, will increase the value of σ'_f mobilised at a given axial strain greater than about 1%. (At axial strains below 1%, increasing the fibre length or width has the opposite effect).

At larger strains, the effect of increasing W_N and L_N in increasing the mobilised deviator stress at a given axial strain is clear in Figures 6 and 7. Figure 7b confirms that longer fibres are only beneficial in this respect if W_N is sufficient to ensure adequate fibre-grain contact across the width of the fibre.

Effects of fibre content - V_{fr} and N_{fg}

Figure 8 shows graphs of deviator stress and volumetric strain against axial strain for (a) $^1/_3$ and (b) $^1/_5$ scaled ballast with different amounts of fibre reinforcement, characterised by volumetric fibre ratios V_{fr} = 0 (unreinforced), 1.6 % and 3.2 %. For both materials, increasing the amount of reinforcement by fibres of given normalised dimensions L_N and W_N delays the occurrence and increases the magnitude of the peak deviator stress, decreases the initial stiffness, reduces dilation and improves ductility. This behaviour is broadly similar to that reported by Michalowski and Cermak (2003), Heineck et al. (2005) and Diambra et al. (2010) for reinforced and unreinforced sand. However, while the mechanical behaviours of reinforced $^1/_3$ and $^1/_5$ scaled ballast follow qualitatively similar trends with increasing V_{fr}, quantitatively the effect of a given amount of fibre reinforcements (i.e. the same V_{fr}) is different in each case. It follows that V_{fr} alone is not an appropriate measure of the amount of fibre reinforcement for the purposes of comparing across grain scales. This may be explained as follows.

At a given V_{fr}, the number of fibres per grain N_{fg} increases with the grain size (Figure 9), because the fibre thickness t_f has not been scaled with D_{50}. Thus as the grain size increases, each individual fibre interacts with fewer grains; and for relatively thin fibres ($D_N = t_f/D_{50} < 0.1$), grain level interactions are the dominant influence on the macro-mechanical behaviour. This explains the greater shear strength at larger axial strains (when the tensile force in the fibres is contributing more significantly to the mobilised strength) exhibited by the $^1/_3$ scaled ballast than the $^1/_5$ scaled ballast specimens in Figure 8.

Better quantitative agreement between the stress ratio (η) and volumetric strain (ε_{vol}) vs axial strain (ε_a) behaviour at the two scales is obtained by comparing data from triaxial tests on specimens having similar N_{fg}, L_N and W_N (Figure 10). This better quantitative agreement is also exhibited when the corrected stress ratio (η'') is plotted against axial strain (ε_a) (Figure 11). As the grain size of the granular material is increased, the number of individual thin strip fibres required to develop similar macro-mechanical behaviour across different scales decreases in proportion. Thus in addition to the relative dimensions of the fibres and grains (Michalowski and Cermak, 2003), the number of individual fibres available for fibre/grain interaction is also important when considering the mechanical behaviour of strip fibre reinforced granular materials across different grain size ranges.

N_{fg} can be changed by changing L_N and W_N as well as by changing V_{fr}. For example, in a fibre reinforced granular material of constant V_{fr}, increasing L_N while W_N remains unchanged (or vice versa) will reduce the value of N_{fg}. Thus making it difficult to investigate the effect of each parameter alone (i.e. L_N and W_N).

Figure 12 shows graphs of deviator stress against axial strain for reinforced specimens having similar L_N and W_N and N_{fg}. In general, there appears to be correlation between the deviator stress and N_{fg}. The variation in deviator stress is about 10 % in Figure 12a and 20 % in Figure 12b, for differences in N_{fg} of about 6% (Figure 12a) and 3% (Figure 12b).

Conclusions

The mechanical properties of fibre reinforced large sized granular materials has been investigated with a particular focus on the relative dimensions of the fibres and the grains and the fibre content, across different grain size ranges. It has been shown that

1. The shear resistance of large grained materials such as scaled railway ballast can be improved by the addition of appropriately sized fibre strips. For each material over the range of stresses considered, the degree of improvement broadly increases with the normalised fibre length and width (L_N and W_N) and the volumetric fibre ratio V_{fr}, subject to certain constraints.

2. The influence of the normalised fibre dimensions is strain dependent. At low strains (~0.1% ≤ ε_a ≤ 1.0%), increasing the normalised fibre width, $W_N = W_f/D_{50}$ reduced the mobilised shear resistance (deviator stress) of the mixture at a given strain. At larger strains, increasing the normalised fibre length $L_N = L_f/D_{50}$ resulted in a higher mobilised shear resistance, provided that the fibres were wide enough to ensure adequate fibre-grain contact.

3. When considering a particular granular material, the volumetric fibre ratio V_{fr} is an adequate measure of the fibre content for interpreting the effect of the reinforcement on the stress-strain-strength behaviour of the mixture. However, V_{fr} is not a suitable basis for comparing the behaviour of reinforced gravels across different grain sizes. For strip fibres of constant thickness that remain thin relative to the grain size, the effectiveness of the fibre reinforcements depends on the number of fibres available to interact

with the grains. Hence the fibre content is better characterised by the numerical fibre:grain ratio N_{fg}, defined as the ratio of the number of fibres N_f to the number of grains N_g.

4. For a full understanding of the effects of fibre reinforcement on scaled railway ballast, the effect of the fibre tension that develops during shear in increasing the normal effective stress on the granular matrix, and hence its resistance to shear stress, must be taken into account. When an appropriate correction is made, the behaviour of the granular matrix in relation to the granular void ratio conforms with conventional soil mechanics principles. Furthermore, almost complete agreement between the stress-strain relationships across scales at a given numerical fibre to grain ratio N_{fg}, relative fibre width W_N and relative fibre length L_N is obtained. This approach also gives insights into the development of fibre tension as a function of N_{fg}, W_N and L_N.

Acknowledgements

This research was supported by the UK Engineering and Physical Sciences Research Council (EPSRC) through the TRACK21 Programme Grant (EP/H044949). The first-named author further acknowledges the support of the Faculty of Engineering and the Environment at the University of Southampton. All data supporting this study are openly available from the University of Southampton repository.

References

Abadi, T. (2015). *Effect of Sleeper and Ballast Interventions on Performance.* PhD. Thesis, University of Southampton.

Abadi, T., Le Pen, L., Zervos, A. & Powrie, W. (2016). Improving the performance of railway tracks through ballast interventions. *Proceedings of the Institution of Mechanical Engineers, Part F: Journal of Rail and Rapid Transit*.

Aingaran, S. (2014). *Experimental investigation of static and cyclic behaviour of scaled railway ballast and the effect of stress reversal.* PhD. Thesis, University of Southampton.

Ajayi, O., Le Pen, L. M., Zervos, A. & Powrie, W. (2016). A behavioural framework for fibre reinforced gravel. *Geotechnique,* (Accepted).

Atkinson, J. H. (2000). Non-linear soil stiffness in routine design. *Géotechnique,* 50(5), 487-508.

Bathurst, R. J. & Raymond, G. P. (1987). Geogrid reinforcement of ballasted track. *Transportation Research Record,* 1153, 8-14.

Diambra, A., Ibraim, E., Russell, A. R. & Wood, D. M. (2013). Fibre reinforced sands: from experiments to modelling and beyond. *International Journal for Numerical and Analytical Methods in Geomechanics,* 37(15), 2427-2455.

Diambra, A., Ibraim, E., Wood, D. M., Bennanni, Y. & Russell, A. R. (2008). Effect of sample preparation on the behaviour of fibre reinforced sands. Proceedings of the 4th International Symposium on Deformation Characteristics of Geomaterials, 2008 Atlanta. 629-636.

Diambra, A., Ibraim, E., Wood, D. M. & Russell, A. R. (2010). Fibre reinforced sands: Experiments and modelling. *Geotextiles and Geomembranes,* 28(3), 238-250.

Dos Santos, A. P. S., Consoli, N. C. & Baudet, B. A. (2010). The mechanics of fibre-reinforced sand. *Geotechnique,* 60(10), 791-799.

Heineck, K. S., Coop, M. R. & Consoli, N. C. (2005). Effect of microreinforcement of soils from very small to large shear strains. *Journal of Geotechnical and Geoenvironmental Engineering, ASCE,* 131(8), 1024-1033.

Indraratna, B., Ngoc Trung, N. & Rujikiatkamjorn, C. (2011). Behavior of geogrid-reinforced ballast under various levels of fouling. *Geotextiles and Geomembranes,* 29(3), 313-322.

Indraratna, B., Nimbalkar, S., Christie, D., Rujikiatkamjorn, C. & Vinod, J. (2010). Field Assessment of the Performance of a Ballasted Rail Track with and without Geosynthetics. *Journal of Geotechnical and Geoenvironmental Engineering, ASCE,* 136(7), 907-917.

Ishikawa, T., Sekine, E. & Miura, S. (2011). Cyclic deformation of granular material subjected to moving-wheel loads. *Canadian Geotechnical Journal,* 48(5), 691-703.

Jewell, R. A. & Wroth, C. P. (1987). Direct shear tests on reinforced sand. *Geotechnique,* 37(1), 53-68.

Koike, Y., Nakamura, T., Hayano, K. & Momoya, Y. (2014). Numerical method for evaluating the lateral resistance of sleepers in ballasted tracks. *Soils and Foundations,* 54(3), 502-514.

Le Pen, L., Bhandari, A. & Powrie, W. (2014). Sleeper End Resistance of Ballasted Railway Tracks. *Journal of Geotechnical and Geoenvironmental Engineering, ASCE,* 140(5).

Le Pen, L., Powrie, W., Zervos, A., Ahmed, S. & Aingaran, S. (2013). Dependence of shape on particle size for a crushed rock railway ballast. *Granular Matter,* 15(6), 849-861.

Lirer, S., Flora, A. & Consoli, N. C. (2011). On the strength of fibre-reinforced soils. *Soils and Foundations,* 51(4), 601-609.

Mcdowell, G. R., Harireche, O., Konietzky, H., Brown, S. F. & Thom, N. H. (2006). Discrete element modelling of geogrid-reinforced aggregates. *Proceedings of the Institution of Civil Engineers-Geotechnical Engineering,* 159(1), 35-48.

Michalowski, R. L. (1997). Limit Stress for Granular Composites Reinforced with Continuous Filaments. *Journal of Engineering Mechanics,* 123(8), 852-859.

Michalowski, R. L. & Cermak, J. (2002). Strength anisotropy of fiber-reinforced sand. *Computers and Geotechnics,* 29(4), 279-299.

Michalowski, R. L. & Cermak, J. (2003). Triaxial compression of sand reinforced with fibers. *Journal of Geotechnical and Geoenvironmental Engineering, ASCE,* 129(2), 125-136.

Michalowski, R. L. & Zhao, A. G. (1996). Failure of fiber-reinforced granular soils. *Journal of Geotechnical Engineering, ASCE,* 122(3), 226-234.

Sadek, S., Najjar, S. S. & Freiha, F. (2010). Shear Strength of Fiber-Reinforced Sands. *Journal of Geotechnical and Geoenvironmental Engineering,* 136(3), 490-499.

Sevi, A. & Ge, L. (2012). Cyclic Behaviors of Railroad Ballast within the Parallel Gradation Scaling Framework. *Journal of Materials in Civil Engineering,* 24(7), 797-804.

Sevi, A. F. (2008). *Physical modeling of railroad ballast using the parallel gradation scaling technique within the cyclical triaxial framework.* PhD Thesis, Missouri Univ. of Science and Technology, Rolla, MO.

Sevi, A. F., Ge, L. & Take, W. A. (2009). A Large-Scale Triaxial Apparatus for Prototype Railroad Ballast Testing. *Geotechnical Testing Journal, ASTM,* 32(4), 297-304.

Tables

Table 1. Typical values of the basic properties of polyethylene fibres (adapted from Ajayi et al., 2016)

	Polyethylene
Specific gravity	0.92
Tensile strength	20.3 MPa[1]; 11.2 MPa[2]
Elastic modulus	0.38 GPa
Softening temperature	85°C
Moisture absorption	< 0.1%

[1] Longitudinal; [2] Transverse relative to the original DPC roll

Table 2. Triaxial test conditions, normalised dimensions of the fibres and grains used and fibre/grain numbers for triaxial test on $^1/_5$ and $^1/_3$ scale ballast specimens

Granular medium	D_{50} (mm)		V_{fr} (%)	e_o	I_D	L_f (mm)	W_f (mm)	L_N	W_N	Avg. N_g	N_f	N_{fg} (%)
			-	0.89[1]	0.03	-	-					
			-	0.83[2]	0.45	-	-					
			-	0.74[3]	0.99	-	-					
$^1/_5$ SB	8	5SB1	1.6	0.82	0.66	58	6	7.1	0.7	10570	256	2.42
		5SB2	1.6	0.82	0.48	58	12	7.1	1.4	10743	138	1.28
		5SB3	1.6	0.83	0.43	58	20	7.1	2.5	10838	82	0.76
		5SB4	3.2	0.88	0.12	58	20	7.1	2.5	10270	146	1.42
		5SB5	6.5	0.97	-0.44	58	20	7.1	2.5	9660	281	2.91
			-	0.87[1]	0.21	-	-					
			-	0.76[3]	0.87	-	-					
$^1/_3$ SB	14	3SB1	1.6	0.79	0.68	50	35	3.6	2.5	2044	54	2.64
		3SB2	1.6	0.79	0.69	50	10	3.6	0.7	1972	189	9.58
		3SB3	1.6	0.80	0.72	100	10	7.1	0.7	2024	96	4.74
		3SB4	1.6	0.80	0.73	100	20	7.1	1.4	2032	48	2.36
		3SB5	1.6	0.79	0.69	100	35	7.1	2.5	2026	27	1.33
		3SB6	3.2	0.91	-0.04	100	35	7.1	2.5	1892	57	3.01

[1] unreinforced loose sample; [2] unreinforced medium dense sample; [3] unreinforced dense sample

Figures

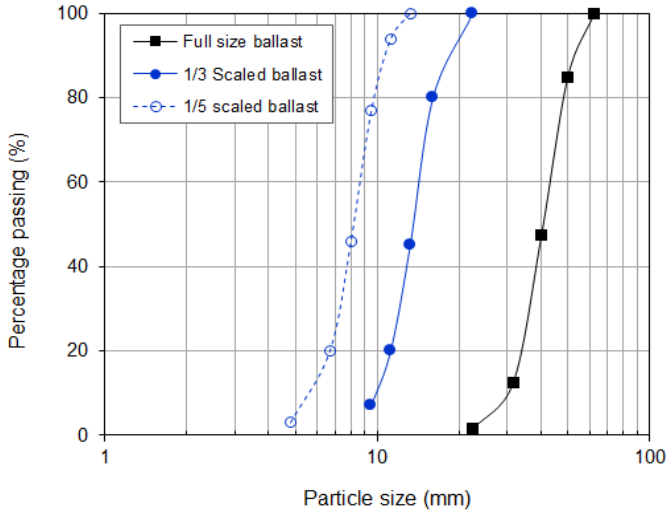

Figure 1. Grain size distribution of $^1/_5$ and $^1/_3$ scaled, and full size ballast (Network Rail specification) (adapted from Ajayi et al., 2016)

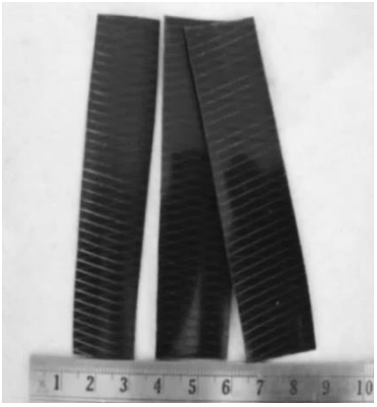

Figure 2. Polyethylene strip fibres used in the triaxial tests (adapted from Ajayi et al., 2016)

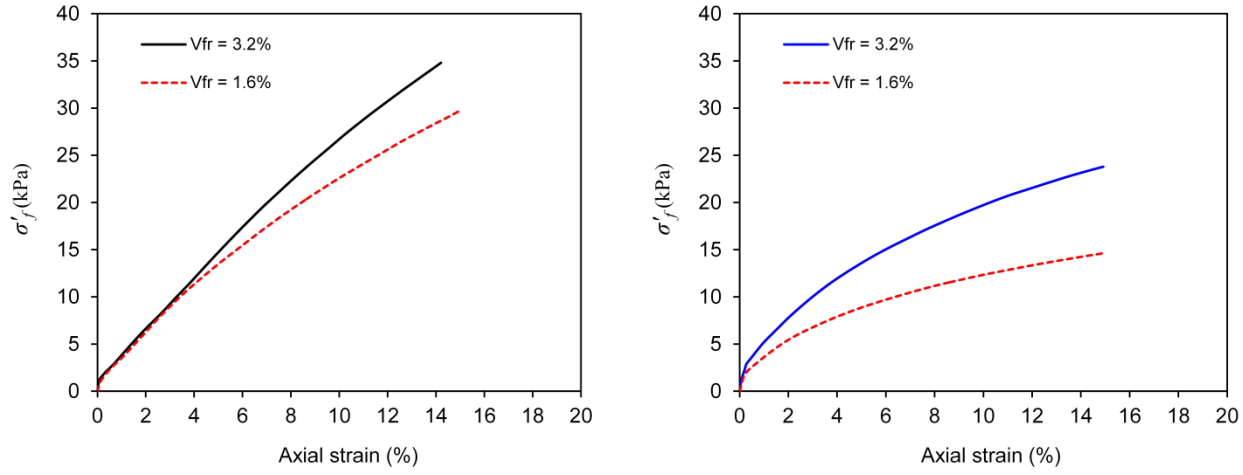

Figure 3. Evolution of additional effective lateral stress, σ'_f, with axial strain for reinforced (a) $^1/_3$ scaled ballast (b) $^1/_5$ scaled ballast specimens with V_{fr} = 1.6 and 3.2 %. L_N = 7.1 and W_N = 2.5.

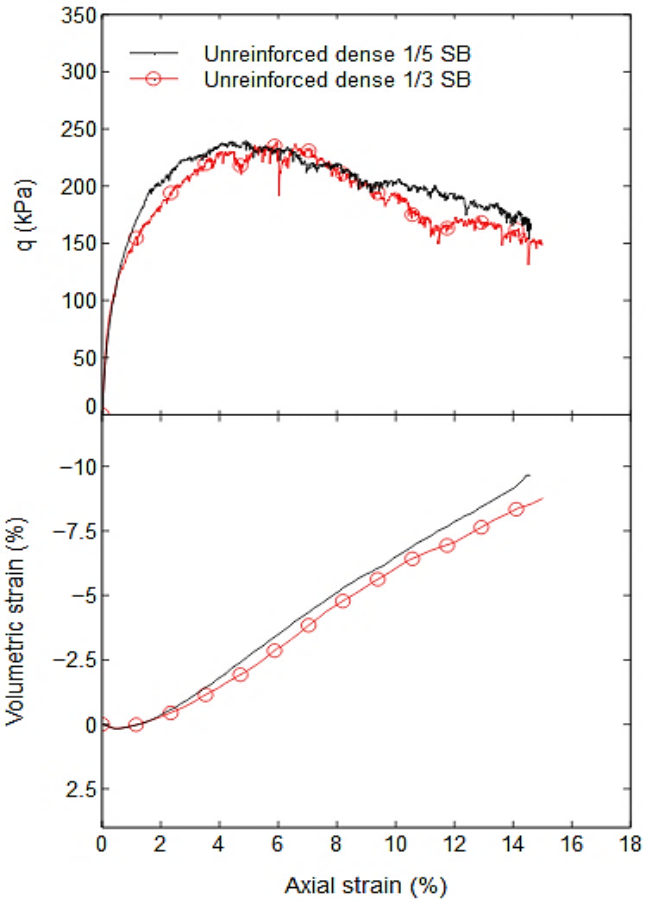

Figure 4. Deviator stress q and volumetric strain ε_{vol} against axial strain ε_a for specimens of unreinforced $^1/_5$ and $^1/_3$ scaled ballast. Cell pressure = 30 kPa

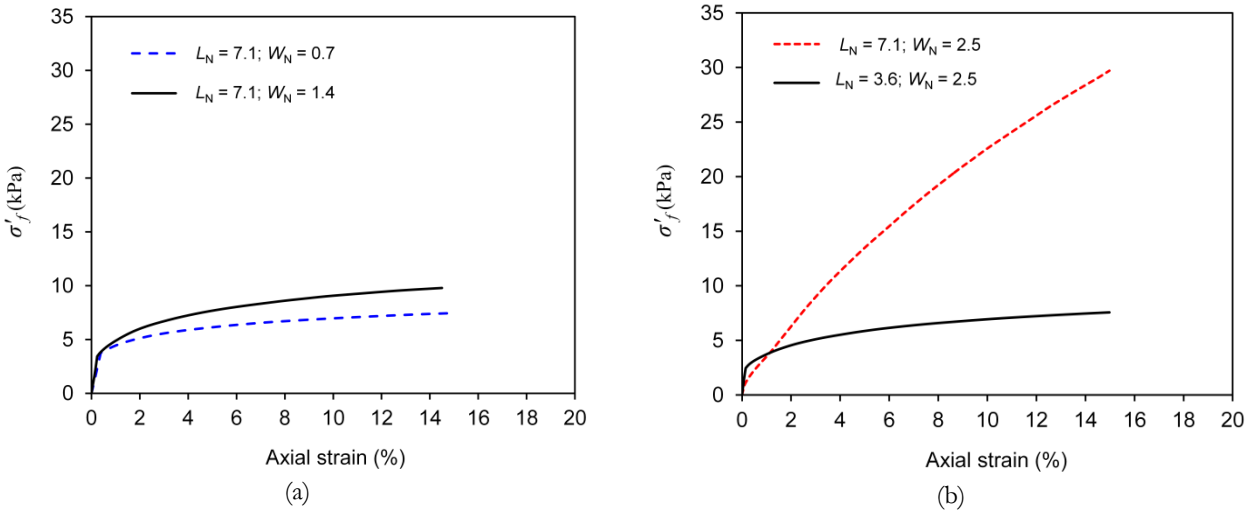

Figure 5. Evolution of additional effective confining stress, σ'_f, with axial strain for reinforced $^1/_3$ scaled ballast specimens with V_{fr}=1.6 % for (a) varying W_N while L_N is constant (b) varying L_N while W_N is constant

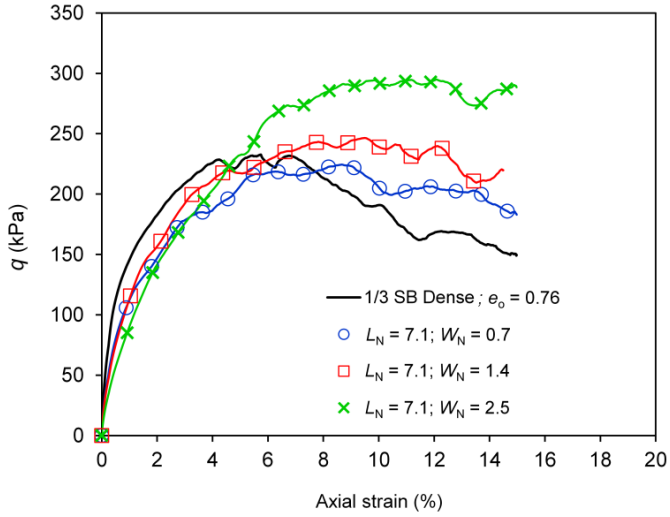

(a)

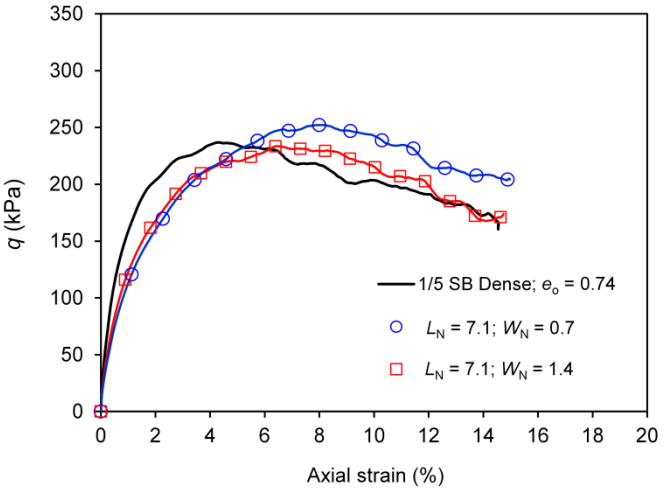

(b)

Figure 6. Effects of varying W_N on the deviator stress, q, of fibre reinforced scaled ballast having V_{fr} = 1.6% and L_N = 7.1 (a) $^1/_3$ scaled ballast (b) $^1/_5$ scaled ballast

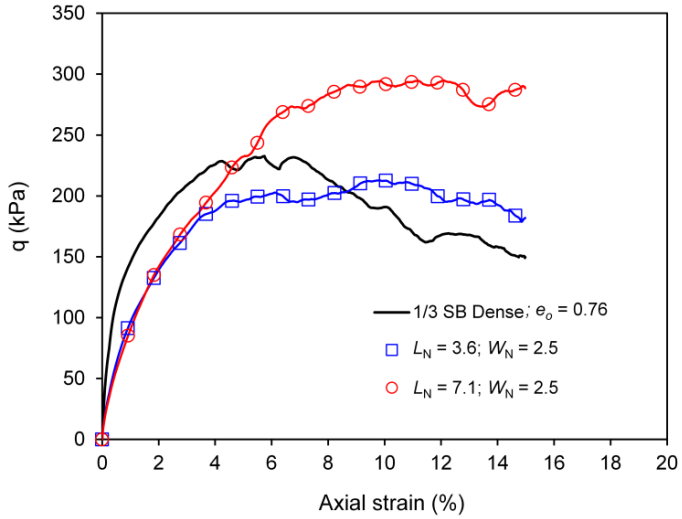

(a)

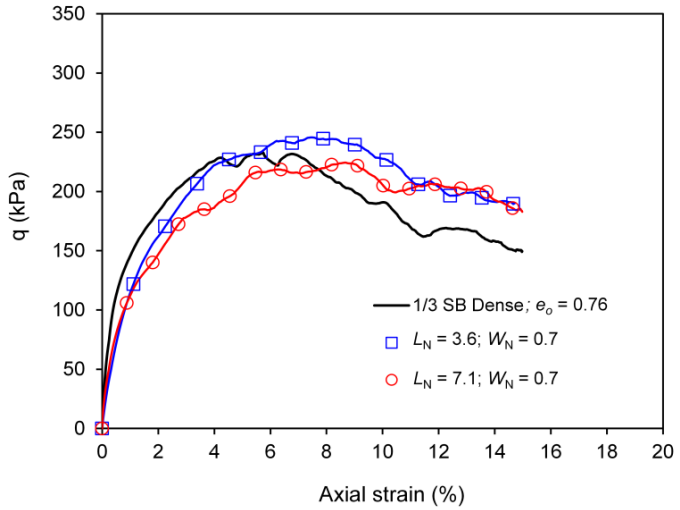

(b)

Figure 7. Effects of varying L_N on the deviator stress, q, of fibre reinforced $^1/_3$ scaled ballast having V_{fr} = 1.6%: (a) W_N = 2.5 (b) W_N = 0.7

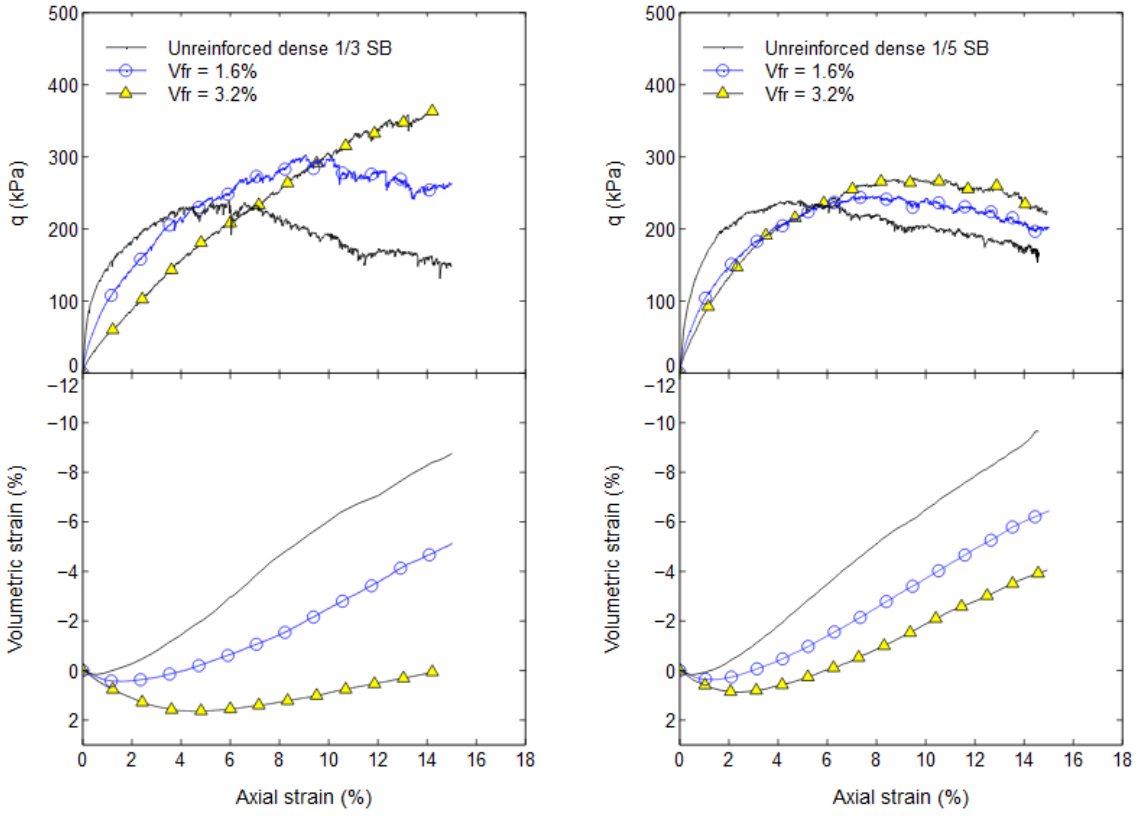

Figure 8. Deviator stress q and volumetric strain ε_{vol} against axial strain ε_a for specimens of (a) $^1/_3$ (b) $^1/_5$ scaled ballast with V_{fr} = 0, 1.6 and 3.2 %. I_N = 7.1 and W_N = 2.5. Cell pressure = 30 kPa

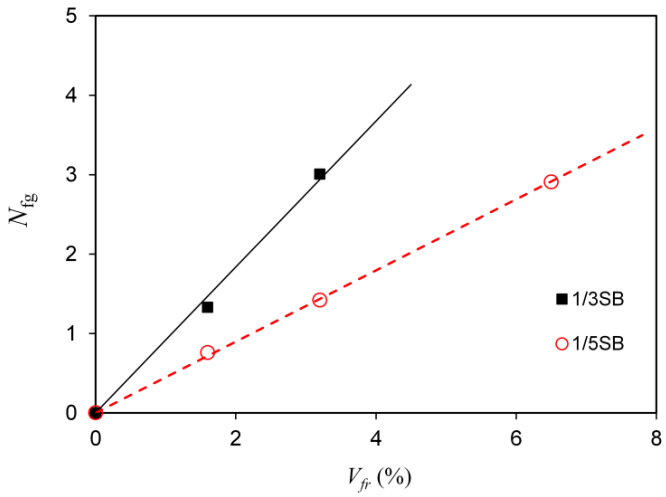

Figure 9. Variation of N_{fg} with increasing V_{fr} for $^1/_3$ and $^1/_5$ scaled ballast

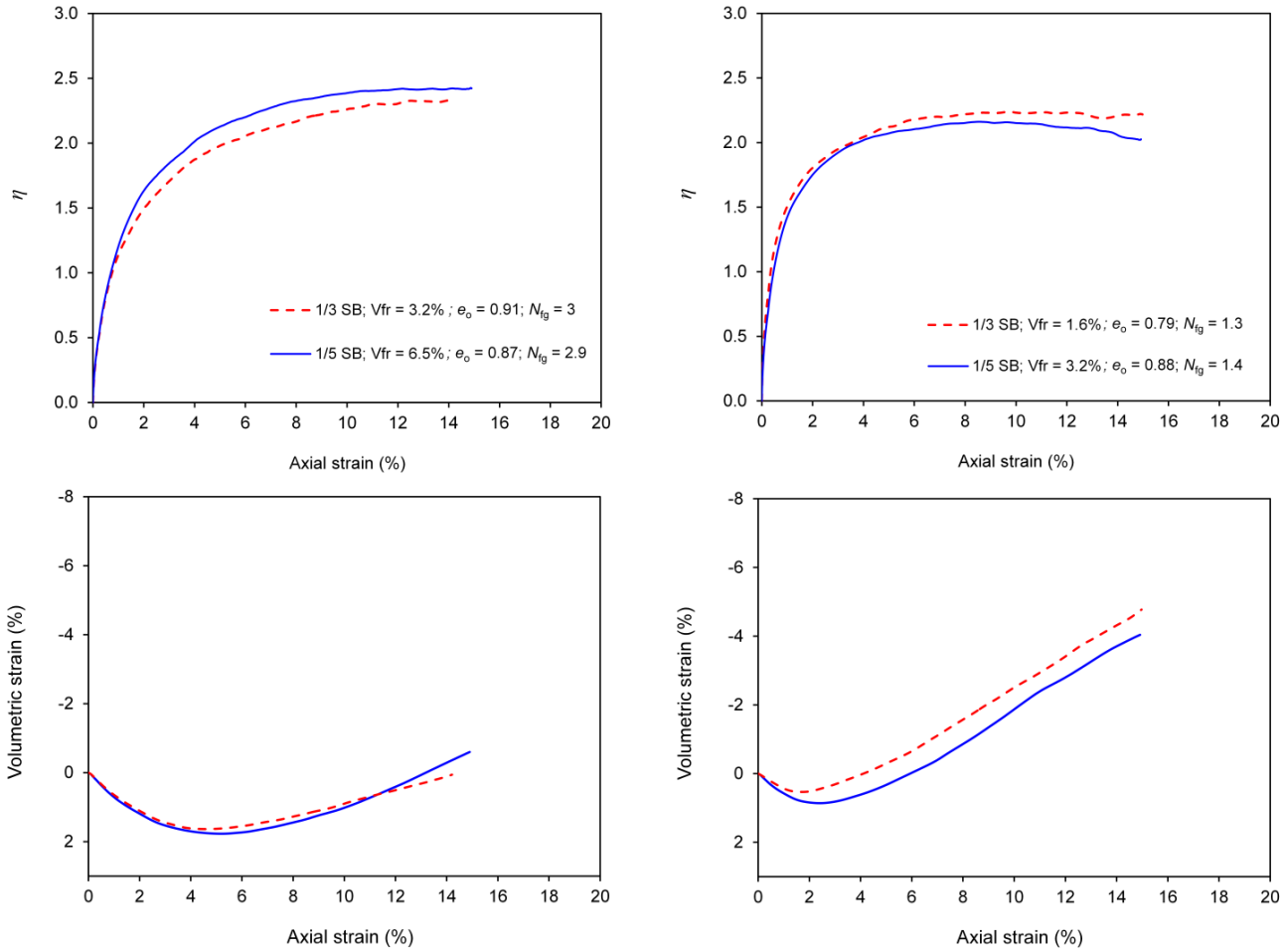

Figure 10. Stress ratio (η) and volumetric strain (ε_{vol}) of reinforced $^1/_3$ and $^1/_5$ scaled ballast specimens at constant $L_N = 7.1$, $W_N = 2.5$ for (a) $N_{fg} \approx 3$ (b) $N_{fg} \approx 1.3$

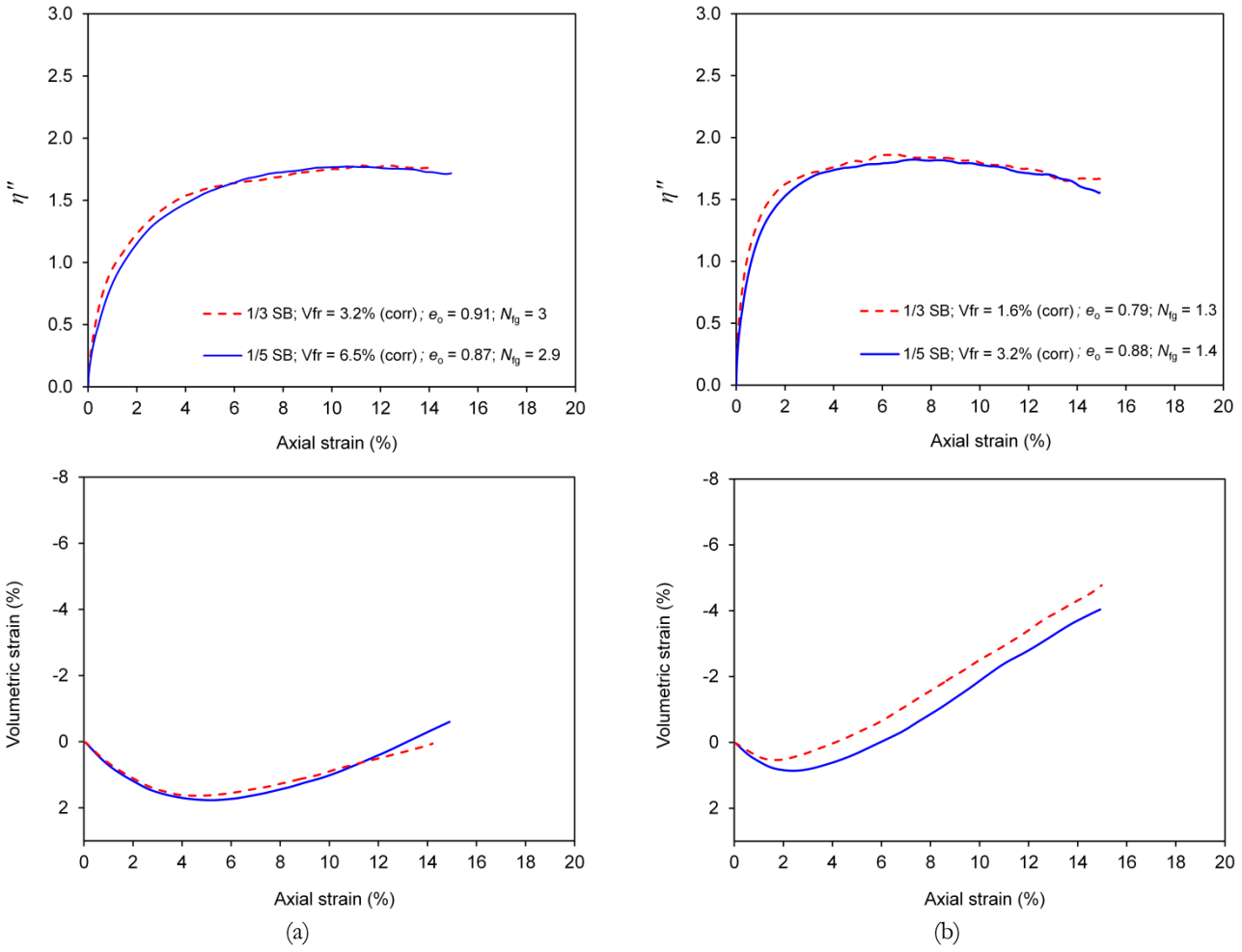

Figure 11. Corrected stress ratio (η'') and volumetric strain (ε_{vol}) of reinforced $^1/_3$ and $^1/_5$ scaled ballast specimens at constant $L_N = 7.1$, $W_N = 2.5$ for (a) $N_{fg} \approx 3$ (b) $N_{fg} \approx 1.3$

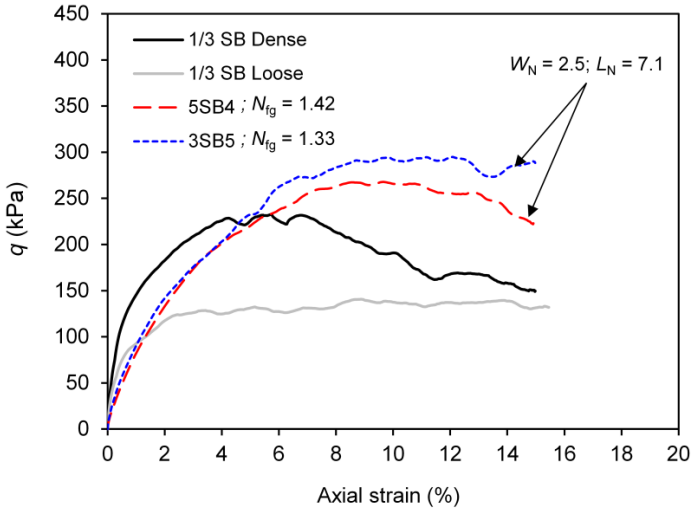

(a)

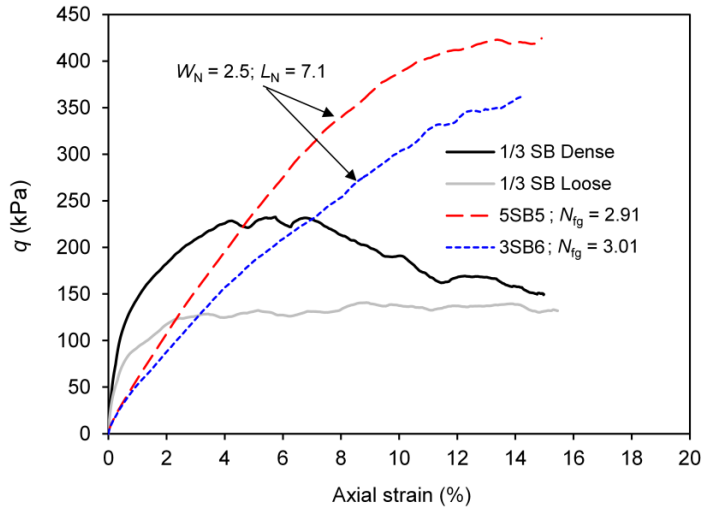

(b)

Figure 12. Deviator stress, q, plotted against axial strain, ε_a, for specimens with constant W_N = 2.5 and L_N = 7.1 for (a) $N_{fg} \approx$ 1.38 (b) $N_{fg} \approx$ 2.96